

See discussions, stats, and author profiles for this publication at: <https://www.researchgate.net/publication/260115799>

On-Chip Separation and Analysis of RNA and DNA from Single Cells

ARTICLE *in* ANALYTICAL CHEMISTRY · FEBRUARY 2014

Impact Factor: 5.64 · DOI: 10.1021/ac4040218 · Source: PubMed

CITATIONS

9

READS

84

5 AUTHORS, INCLUDING:



[Hirofumi Shintaku](#)

Kyoto University

35 PUBLICATIONS 224 CITATIONS

[SEE PROFILE](#)



[Hidekazu Nishikii](#)

Stanford University

28 PUBLICATIONS 299 CITATIONS

[SEE PROFILE](#)



[Lewis Anthony Marshall](#)

Purigen Biosystems

10 PUBLICATIONS 122 CITATIONS

[SEE PROFILE](#)



[Juan G Santiago](#)

Stanford University

307 PUBLICATIONS 10,524 CITATIONS

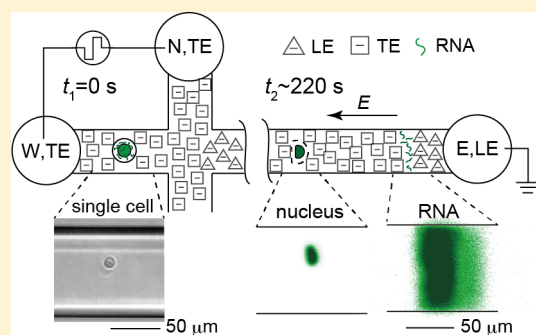
[SEE PROFILE](#)

On-Chip Separation and Analysis of RNA and DNA from Single Cells

Hirofumi Shintaku,^{†,||} Hidekazu Nishikii,[‡] Lewis A. Marshall,[§] Hidetoshi Kotera,^{||} and Juan G. Santiago^{*,†}[†]Department of Mechanical Engineering, [‡]Divisions of Blood and Marrow Transplantation, and [§]Department of Chemical Engineering, Stanford University, Stanford, California 94305, United States^{||}Department of Micro Engineering, Kyoto University, Kyoto 606-8501, Japan

S Supporting Information

ABSTRACT: The simultaneous analysis of RNA and DNA of single cells remains a challenge as these species have very similar physical and biochemical properties and can cross-contaminate each other. Presented is an on-chip system that enables selective lysing of single living cells, extraction, focusing, and absolute quantification of cytoplasmic RNA mass and its physical separation from DNA in the nucleus using electrical lysing and isotachopheresis (ITP). This absolute quantitation is performed without enzymatic amplification in less than 5 min. The nucleus is preserved, and its DNA fluorescence signal can be measured independently. We demonstrate the technique using single mouse lymphocyte cells, for which we extracted an average of 14.1 pg of total RNA per cell. We also demonstrate correlation analysis between the absolute amount of RNA and relative amount of DNA, showing heterogeneity associated with cell cycles. The technique is compatible with fractionation of DNA and RNA and with downstream assays of each.



Analysis of RNA and DNA at the single cell level is crucial to the understanding of the heterogeneity within cell populations, and new tools for this work are just emerging.¹ Recent progress in microfluidics has revolutionized the area and created new capabilities for single cell analysis.² For example, Marcus et al.³ demonstrated an integrated microfluidic chip that performed single cell lysis, RNA purification, and complementary DNA (cDNA) synthesis. Since then, the technique has been improved⁴ and similar techniques have been used to measure the single cells.⁵ The technique is now well established but requires a specialized system for the manipulation (e.g., pumping liquids and valving). Further, the basic idea of quantifying the amount of RNA has relied upon its conversion to cDNA and subsequent amplification by enzymatic processes such as quantitative polymerase chain reaction (qPCR). Such basic approaches are effective but may not be optimal, as PCR is well-known to introduce sequence-specific bias.¹ Because of this, most findings require validation by in situ hybridization or staining.

Capillary electrophoresis (CE) methods using both traditional free-standing capillaries and on-chip CE have also been used for handling and analyzing molecules from single cells.⁶ However, few studies have focused on direct detection of RNA without amplification. Han and Lillard⁷ demonstrated direct measurement of RNA from a single cell and obtained an electropherogram of rRNA. They performed cell lysis inside the same capillary used for separation using sodium dodecyl sulfate (SDS). Their protocol separated RNA by CE and quantified RNA using an ethidium bromide label and laser-induced fluorescence detection. In subsequent work, Lillard's group examined RNA expression in various phases of the cell cycle

(G₁, S, G₂, and M) and reported changes of the total amount of RNA and individual RNA sequences over each phase.⁸ Their limit of detection of CE was well below the single cell level. However, their protocol provided only the relative amount of the RNA and no simultaneous RNA and DNA information.

A single mammalian cell contains approximately 10–40 pg of RNA, as determined from averages based on a larger number of cells.^{9–12} or from single cells.¹³ However, these methods for quantification used time-consuming and labor-intensive steps for lysing, extraction of RNA, and buffer exchange(s). We know of no reports of miniaturized systems that can directly lyse and quantify the absolute amount of total RNA from a single cell. We also know of no absolute quantitation of RNA with simultaneous measurement of DNA relative abundance. In this technical note, we offer a new combination of on-chip electrical lysis and ITP that can be used to isolate single live cells; lyse them; and extract, concentrate, and measure total cytoplasmic RNA and nuclear DNA individually, all within 5 min. Focusing RNA into an ITP interface makes the process robust to dispersion and is compatible with integration with downstream analysis such as a CE and cDNA hybridization based assay.^{14–16}

ITP is an electrophoretic technique that can focus target analytes at the ITP interface between a low mobility trailing (TE) and a high mobility leading electrolytes (LE). We have demonstrated ITP extraction of RNA and DNA from cell culture,¹⁷ whole blood,^{18–20} and urine lysates.²¹ ITP offers highly sensitive,^{15,22,23} robust,²⁴ rapid,²¹ and extremely

Received: December 11, 2013

Accepted: January 24, 2014

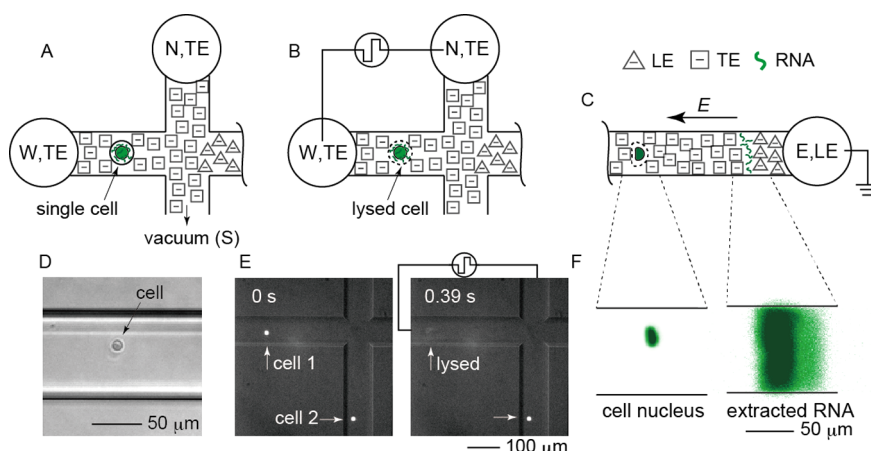


Figure 1. Schematic of single cell RNA extraction and quantification method. (A) Single cells were introduced from the W reservoir and isolated in the injection channel by applying vacuum. (B) Each cell was electrically lysed by a bipolar voltage pulse applied between the N and the W reservoirs. (C) Total cytoplasmic RNA from the lysed cell was extracted and accumulated within the ITP interface. Remaining cell debris (including the nucleus) was separated from the RNA. (D) A bright field image of isolated single cell in the injection channel. (E) Lysing of individual cells. Cells 1 and 2 are, respectively, within and outside the lysing electric field. Only cell 1 is lysed. (F) Typical experimental images of cell nucleus (left behind) and extracted RNA from a single cell at the ITP interface (using different color scales for clarity).

selective^{25,26} sample preparation and it is possible to preconcentrate analytes by as much as 10^6 -fold.²⁷ We recently reviewed ITP extraction of RNA and DNA.²⁸

In the current work, we focus on a single cell assay and present a protocol that uses electric fields to control the entire process in a standard fluidic chip with no moving parts and only end-channel electrodes after initial isolation of a single cell. We demonstrate manipulation and controlled single cell lysing followed by selective extraction of RNA via ITP from the lysed single cell cytoplasm. We also demonstrate absolute quantification of RNA and correlation analysis with a semiquantitative DNA amount from a single cell. The results show that our protocol is a practical method to access heterogeneity in the amount of RNA and DNA in single cells.

MATERIALS AND METHODS

Overview of Single Cell Assay. Figure 1A–C show a schematic representation of our assay. We used an off-the-shelf microfluidic chip with a cross geometry (model NS12A, Caliper Life Sciences, CA). The microfluidic chip consists of borosilicate glass microchannels of $90\ \mu\text{m}$ wide and $20\ \mu\text{m}$ deep (see Figure S-1A in the Supporting Information). We prefilled the microchannel with LE buffer and added a $2\ \mu\text{L}$ cell suspension (approximately $5\ \text{cells}/\mu\text{L}$) in TE buffer into the west (W) reservoir. We introduced individual cells from this low concentration solution by applying a vacuum to the south (S) reservoir. Once we visually confirmed a single cell was isolated in the injection channel, between the W reservoir and the cross-junction, we removed the vacuum and added $20\ \mu\text{L}$ of the TE buffer to the W and north (N) reservoirs. We placed platinum wire electrodes into the W, N, and east (E) reservoirs, and applied voltage to the electrodes using a high voltage sequencer (HVS448 3000D, LabSmith). We first applied a bipolar voltage pulse between the W and N reservoirs (each pulse $100\ \text{ms}$ wide, $3000\ \text{V}$ magnitude) to lyse the single cell. We then immediately initiated ITP by applying a dc electric field and extracted RNA from the lysed cell. The voltage sequence is shown schematically in Figure S-1B in the Supporting Information. RNA simultaneously complexes with

SYBR Green II mixed homogeneously into the LE, and we detect it $40\ \text{mm}$ downstream of the cross-junction.

ITP Chemistry. The LE was $50\ \text{mM}$ Tris and $25\ \text{mM}$ HCl containing 0.4% a poly(vinylpyrrolidone) (PVP) and $1\times$ SYBR Green II (calculated pH of 8.1). The TE was $50\ \text{mM}$ Tris and $25\ \text{mM}$ HEPES containing (initial calculated pH of 8.3) 0.4% PVP. We included PVP to both suppress electroosmotic flow and separate the extracted RNA from the cell debris via the sieving effect of PVP (see the Supporting Information section S-2 for selection of an appropriate PVP concentration). We obtained Tris, HEPES, and HCl from Sigma-Aldrich (St. Louis, MO), SYBR Green II from Invitrogen (Carlsbad, CA), and PVP (MW $1\ \text{MDa}$) from Acros Organics (Thermo Fisher Scientific, NJ). We prepared all solutions in UltraPure DNase-/RNase-free deionized (DI) water (Life Technologies, Carlsbad, CA).

Cell Preparation. We cultured the A20 cell line (mouse lymphocyte cells) in RPMI-1640 Medium (Life Technologies, Carlsbad, CA) with 10% fetal bovine serum and 1% penicillin-streptomycin-glutamine at $37\ ^\circ\text{C}$ in $5\% \text{CO}_2$. We washed the cells with phosphate buffered saline once and suspended in a sample buffer solution containing $50\ \text{mM}$ Tris, $25\ \text{mM}$ HEPES, and $175\ \text{mM}$ sucrose at the concentration of $\sim 5\ \text{cells}/\mu\text{L}$ and stored on ice until the experiments were performed. We added $175\ \text{mM}$ sucrose to the sample buffer to compensate for the osmotic pressure and to preserve the cell viability until the lysis. We confirmed the sample buffer did not have a significant adverse effect on cell viability for at least $3\ \text{h}$ (see Figure S-2 in the Supporting Information). In all cases, we used cell samples prepared within $3\ \text{h}$ or less.

Channel Preparation. Figure S-1A in the Supporting Information shows the geometry of the microfluidic chip. Prior to each experiment, we preconditioned the microchannel by filling E and S reservoirs and applying vacuum at N and W reservoirs using a single split vacuum line. We used the following cleaning chemistry: $1\ \text{M}$ NaOH for $10\ \text{min}$, deionized (DI) water for $3\ \text{min}$, and then dried by applying vacuum to the W and N reservoirs for $1\ \text{min}$. Following this, we filled the E and S reservoirs with the LE solution and applied vacuum at the

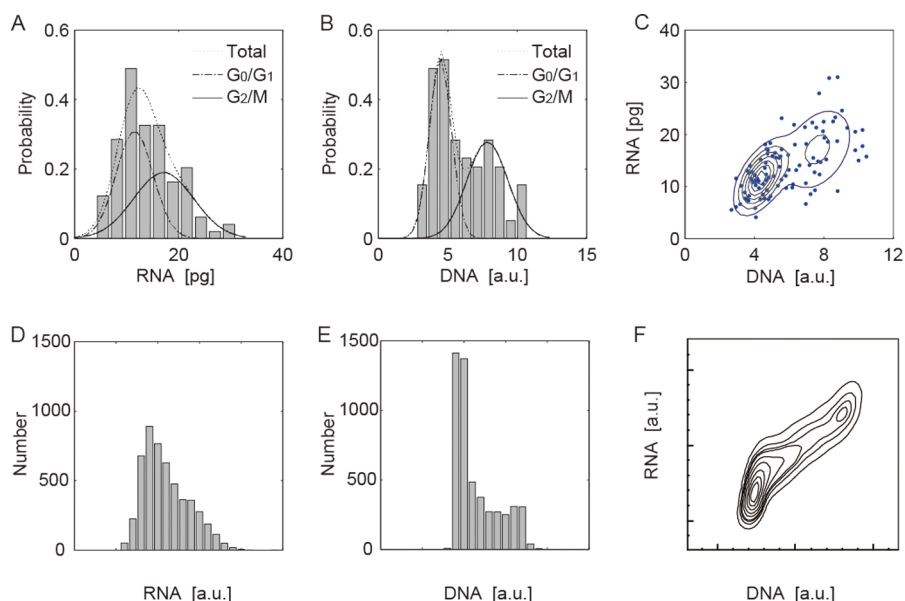


Figure 2. Statistics on measurements of RNA and DNA from individual single cells. Parts A–C summarize data from our method, and parts D–F show FACS data for comparison. (A) Histogram of absolute amount of extracted RNA masses. (B) Histogram of relative amount of DNA. (C) Relation between the absolute amount of RNA and relative amount of DNA from living single cells. The contour lines show the result of two-dimensional Gaussian analysis. (D) Histogram of relative amount of RNA by FACS. (E) Histogram of relative amount of DNA by FACS. (F) The contour lines show the correlation between RNA and DNA.

N and W reservoirs to fill the microchannel for approximately 1.5 min.

Visualization. We performed on-chip visualizations of the extracted RNA using an inverted epifluorescence microscope (Eclipse TS100, Nikon) equipped with a 20X objective (UPlanFI), a blue LED (LEDC7, Thor Laboratories, Newton, NJ), a filter cube (XF23, Omega optical, VT), and 0.6 \times demagnification lens (TV Lens C-0.6 \times , Nikon). We acquired images with a CCD camera (MicroMAX-1300Y, Princeton Instruments) with 100 ms exposure time and 2 \times 2 binning.

RESULTS AND DISCUSSION

Controlled Electrical Lysis of Single Cell. We observed a living single cell isolated in the injection channel as approximately spherical body with a diameter ranging from 10 to 15 μ m (Figure 1D). In all experimental runs, we visually confirmed the presence and the viability of a single cell in the injection channel. Our injection protocol and end-channel electrodes only lyse cells placed in the injection channel (see the Supporting Information section S-1). The cell lysing process was very repeatable and showed 100% yield across all observations.

Dynamics of ITP and Cell Nucleus. Our application of a dc electric field immediately upon completion of the lysing pulse resulted in rapid ITP focusing of the RNA from individual cells. Figure 1F shows representative images of extracted RNA in the ITP interface from a single cell. We obtained this image 220 s from the time of cell lysis. We defined the signal-to-noise ratios (SNR) of the RNA fluorescence in the ITP zone as the fluorescence intensity above the background divided by the standard deviation among negative controls. Our mean SNR was 7.6 and the minimum SNR was 1.5.

All experiments resulted in a focused RNA zone in ITP and a trailing ellipsoidal body we attributed to a cell nucleus (see Figure 1F). We confirmed this attribution through a series of experiments using Hoechst 33342 dye (B2261, Sigma-Aldrich,

which is selective to DNA vs RNA) and using RNase (RNase A, QIAGEN) (see section S-2 of the Supporting Information). The nuclei migrated in the same direction as the ITP interface, indicating a net negative charge, but the drift velocity of the nuclei varied significantly among experimental runs. We attribute this variation to variations in size and morphology and other differences (e.g., number and ionization states of surface proteins). In contrast, the ITP-focused zone always remained in motion at drift velocities expected from the ITP dynamics.²⁹

Quantification of Absolute Amount of RNA and Relative Amount of DNA. We performed 100 experiments where we lysed single cells, separated nuclei from total cytoplasmic RNA, focused and quantified cytoplasmic RNA, and obtained relative measures of total DNA in individual nuclei. We used a calibration curve constructed using experiments with spiked synthetic RNA (0.5–10 Kb RNA Ladder, Invitrogen) to quantify the absolute amount of RNA in ITP interface using integrated intensity (see the Supporting Information section S-3). Figure 2A shows a histogram for measured absolute RNA masses. See also Figure S-5B in the Supporting Information for RNA data ordered chronologically versus the experimental run. The histogram showed a most frequent value of about 11.0 pg and a mean of 14.1 pg. These measures are consistent with reported total RNA from single mammalian cells.¹⁰ The standard deviation normalized by the mean value was 39% (significantly larger than the 12% value observed among runs in the calibration data, see the Supporting Information section S-3). The magnitude of the variation relative to variation within repeats of the calibration leads us to conclude that the large observed variation in our cell data is due to cell population heterogeneity (see further discussion below).

In all of these experiments, we integrated the fluorescence intensity of the cell nucleus as an additional, correlated measurement specific to each cell (see the details of the image analysis in the Supporting Information section S-4). As

we discussed in Supporting Information section S-2, we confirmed our protocol extracts only cytoplasmic RNA from the lysed cell and keeps DNA in the nucleus. We hypothesize that the integrated fluorescence intensity from the cell nucleus provides a measure of the relative amount of DNA. The statistical correlation between RNA and DNA amounts and the good qualitative comparison to our FACS data help support this hypothesis as described below. The relative amount of DNA also showed large variation with a standard deviation normalized by mean of 34% (significantly larger than estimated measurement uncertainties, see Figure 2B). The DNA amount distribution showed two distinct peaks: The first at about 4.5 au and the second at about 7.8 au (1.7 ratio of the local maxima). We attribute these two peaks to the G_0/G_1 and G_2/M cell phases,³⁰ where single cells contain single and double copies of DNA, respectively. The cell sample was a mixture of proliferating and nonproliferating cells (G_0 phase). Proliferating cells pass through four cell phases, the G_1 , S, G_2 , and M phases, and synthesize DNA in the S phase. We therefore hypothesize that the ratio between local maxima in the histogram was smaller than 2 because of the contribution by the S phase.

Correlation Analysis between RNA and DNA. We examined the correlation between the absolute amount of the RNA and the relative amount of DNA as shown in Figure 2C. We observed a significant correlation with a positive coefficient of 0.62 (a p value of 5.5×10^{-12} for the null hypothesis of no observed correlation). The positive coefficient indicates that the greater amount of DNA coincides with the greater amount of the RNA. We thus attribute the variation in each measure to the cell cycle but not to the extraction efficiency of RNA. See also the Supporting Information section S-5 for more details.

We also performed an analysis based on the fitting of two-dimensional Gaussian distributions to the data in Figure 2 C. We observed the best fitting result with two two-dimensional Gaussians, suggesting that the 100 single cells originate from two distinct populations (see also the Supporting Information section S-5). We show the projection of the two-dimensional fitting as lines in Figure 2A,B. In Figure 2B, we found that each population captures the two distinct peaks, respectively. This supports the conclusion that we observe two distinct populations associated with the G_0/G_1 and G_2/M phases. We also observed a consistent fitting result for the amount of extracted RNA, as shown in Figure 2A.

Comparison to FACS Data. We further evaluated our technique by performing analysis on cells from the same cell culture with a fluorescence activated cell sorter (FACS). We used a protocol using Pyronin Y and Hoechst 33342 of fluorescent dyes³⁰ for RNA and DNA relative quantification, respectively (see Supporting Information section S-6 for the detailed protocol). We summarize the FACS analysis in Figure 2D–F. We observed good qualitative agreement between our assay and FACS. We found that the measurements of relative RNA and relative DNA amounts provided by FACS also show correlated, bimodal distributions, as with our data. The correlation diagram of Figure 2F was obtained from 5109 cells and so shows more details than our assay. FACS is a mature, high-throughput technique and so offers a much larger number of measurements. However, unlike FACS, our assay provides absolute quantitation of RNA and further physically lyses and separates DNA from RNA on chip. By combining RNase control into single ITP chemistry,²⁰ the latter is advantageous for integration with downstream analysis such as CE and cDNA hybridization based assay.^{14–16} In contrast,

the relative DNA and relative RNA quantities obtained with FACS cannot be preserved, fractionated, and made available for individual analyses. We hope to further automate our method in the future to increase the number of cells analyzed and integrate further downstream correlated analyses.

CONCLUSION

We developed an electrokinetic method for rapid and selective lysing; separation of cytoplasmic RNA from nucleus DNA; collection, focusing, and absolute quantification of RNA; and simultaneous relative quantification of DNA from living single cells. Our method uses on-chip electrical lysis and RNA extraction via ITP with optimized chemistry to separate individual cell nuclei from RNA. We analyze both RNA and DNA with no amplification. We show an initial demonstration of our technique in quantitation of 100 individual cells. Analyses show a positive correlation between absolute RNA amount and relative DNA amounts. The correlated bimodality of the DNA and RNA amounts suggests cells were analyzed in mostly the G_0/G_1 or the G_2/M cell phases.

We also performed comparisons between our data and FACS data on the same cell line. FACS data confirms our observations regarding correlation between DNA and RNA amounts and also suggest two major populations of cells corresponding to the phases described above. Unlike FACS, our technique obtains absolute RNA quantitation, physically lyses cells, and separates RNA from DNA. The approach also creates the opportunity to fractionate and deliver DNA and RNA to other downstream correlated analyses. Such analyses may be useful in the analysis of highly heterogeneous cell populations such as solid tumors.³¹ We hope to demonstrate such additional integration and automate our assay to include full electric field control of cells, RNA, and nuclei and image-analysis-based cell identification and control.

ASSOCIATED CONTENT

Supporting Information

Additional information as noted in text. This material is available free of charge via the Internet at <http://pubs.acs.org>.

AUTHOR INFORMATION

Corresponding Author

*E-mail: juan.santiago@stanford.edu.

Notes

The authors declare no competing financial interest.

REFERENCES

- (1) Kalisky, T.; Blainey, P.; Quake, S. R. *Annu. Rev. Genet.* **2011**, *45*, 431–445.
- (2) Zare, R. N.; Kim, S. *Annu. Rev. Biomed. Eng.* **2010**, *12*, 187–201.
- (3) Marcus, J. S.; Anderson, W. F.; Quake, S. R. *Anal. Chem.* **2006**, *78*, 3084–3089.
- (4) White, A. K.; VanInsberghe, M.; Petriv, O. I.; Hamidi, M.; Sikorski, D.; Marra, M. A.; Piret, J.; Aparicio, S.; Hansen, C. L. *Proc. Natl. Acad. Sci. U.S.A.* **2011**, *108*, 13999–14004.
- (5) Zhong, J. F.; Chen, Y.; Marcus, J. S.; Scherer, A.; Quake, S. R.; Taylor, C. R.; Weiner, L. P. *Lab Chip* **2008**, *8*, 68–74.
- (6) Borland, L. M.; Kottegoda, S.; Phillips, K. S.; Allbritton, N. L. *Annu. Rev. Anal. Chem.* **2008**, *1*, 191–227.
- (7) Han, F.; Lillard, S. J. *Anal. Chem.* **2000**, *72*, 4073–4079.
- (8) Han, F.; Lillard, S. J. *Anal. Biochem.* **2002**, *302*, 136–143.
- (9) Ogura, M.; Agata, Y.; Watanabe, K.; McCormick, R. M.; Hamaguchi, Y.; Aso, Y.; Mitsuhashi, M. *Clin. Chem.* **1998**, *44*, 2249–2255.

- (10) Wen, J.; Legendre, L. A.; Bienvenue, J. M.; Landers, J. P. *Anal. Chem.* **2008**, *80*, 6472–6479.
- (11) Schmid, A.; Kortmann, H.; Dittrich, P. S.; Blank, L. M. *Curr. Opin. Biotechnol.* **2010**, *21*, 12–20.
- (12) Uemura, E. *Brain. Res. Bull.* **1980**, *5*, 117–119.
- (13) Roozmond, R. C. *Histochem. J.* **1976**, *8*, 625–638.
- (14) Bahga, S. S.; Chambers, R. D.; Santiago, J. G. *Anal. Chem.* **2011**, *83*, 6154–6162.
- (15) Eid, C.; Garcia-Schwarz, G.; Santiago, J. G. *Analyst* **2013**, *138*, 3117–3120.
- (16) Garcia-Schwarz, G.; Santiago, J. G. *Angew. Chem., Int. Ed.* **2013**, *125*, 11748–11751.
- (17) Schoch, R. B.; Ronaghi, M.; Santiago, J. G. *Lab Chip* **2009**, *9*, 2145–2152.
- (18) Persat, A.; Marshall, L. A.; Santiago, J. G. *Anal. Chem.* **2009**, *81*, 9507–9511.
- (19) Marshall, L. A.; Han, C. M.; Santiago, J. G. *Anal. Chem.* **2011**, *83*, 9715–9718.
- (20) Rogacs, A.; Qu, Y. T.; Santiago, J. G. *Anal. Chem.* **2012**, *84*, 5858–5863.
- (21) Bercovici, M.; Kaigala, G. V.; Mach, K. E.; Han, C. M.; Liao, J. C.; Santiago, J. G. *Anal. Chem.* **2011**, *83*, 4110–4117.
- (22) Jung, B. G.; Zhu, Y. G.; Santiago, J. G. *Anal. Chem.* **2007**, *79*, 345–349.
- (23) Bahga, S. S.; Kaigala, G. V.; Bercovici, M.; Santiago, J. G. *Electrophoresis* **2011**, *32*, 563–572.
- (24) Bocek, P. *Analytical Isotachophoresis*; VCH : Weinheim, Germany, 1988.
- (25) Persat, A.; Chivukula, R. R.; Mendell, J. T.; Santiago, J. G. *Anal. Chem.* **2010**, *82*, 9631–9635.
- (26) Persat, A.; Santiago, J. G. *Anal. Chem.* **2011**, *83*, 2310–2316.
- (27) Jung, B.; Bharadwaj, R.; Santiago, J. G. *Anal. Chem.* **2006**, *78*, 2319–2327.
- (28) Rogacs, A.; Marshall, L. A.; Santiago, J. G. *J. Chromatogr., A* **2014**, DOI: 10.1016/j.chroma.2013.12.027.
- (29) Bercovici, M.; Lele, S. K.; Santiago, J. G. *J. Chromatogr., A* **2009**, *1216*, 1008–1018.
- (30) Crissman, H. A.; Darzynkiewicz, Z.; Tobey, R. A.; Steinkamp, J. A. *Science* **1985**, *228*, 1321–1324.
- (31) Gerlinger, M.; Rowan, A. J.; Horswell, S.; Larkin, J.; Endesfelder, D.; Gronroos, E.; Martinez, P.; Matthews, N.; Stewart, A.; Tarpey, P.; Varela, I.; Phillimore, B.; Begum, S.; McDonald, N. Q.; Butler, A.; Jones, D.; Raine, K.; Latimer, C.; Santos, C. R.; Nohadani, M.; Eklund, A. C.; Spencer-Dene, B.; Clark, G.; Pickering, L.; Stamp, G.; Gore, M.; Szallasi, Z.; Downward, J.; Futreal, P. A.; Swanton, C. *N. Engl. J. Med.* **2012**, *366*, 883–892.